shift φ between the transverse polarizations of the helium metastable state and of the excited ionic state is measured as a function of the applied static field. Equation (13) is then used to extract the lifetime τ_J of the ionic state.

If the transverse polarization of the helium metastable atoms were stationary, the predicted effect would be the spin analog of the Hanle effect.[7] Thus, we can view the system described here as the equivalent of the Hanle effect in a reference frame rotating at the precession frequency of the helium metastable atoms.

Although the analysis of systems not satisfying the conditions imposed in this paper could be more difficult, we expect that the general properties and, in particular, the transfer of electronic polarization observed in the example would not differ substantially from those obtained here. Considering the example, we feel that Penning-ionizing collisions will prove to be an important tool in the area of ion spectroscopy.

Appendix.—In carrying out the calculations, a number of traces over products of spin and orbital angular momentum operators are encountered. It is convenient to use eigenstates of spin and orbital angular momentum rather than total angular momentum. In this case the pertinent traces decompose into products of a trace over spin states and a trace over orbital angular momentum states. The traces of particular interest are

$$\mathrm{Tr}_l \hat{L}_i = 0, \quad \mathrm{Tr}_l 1 = 2l+1,$$
$$\mathrm{Tr}_l \hat{L}_i \hat{L}_j = \tfrac{1}{3}\delta_{ij} l(l+1)(2l+1),$$
$$\mathrm{Tr}_l \hat{L}_i \hat{L}_j \hat{L}_k = \tfrac{1}{6} i\epsilon_{ijk} l(l+1)(2l+1),$$

where $l = \frac{1}{2}$ ($\hat{L}_i = \hat{S}_i$) for the spin states and $l = L$ for the orbital angular momentum states.

*Research supported in part by the U. S. Office of Naval Research under Contract No. ONR-NOOO14-69-A-0141-0004.

[1]W. Happer, Rev. Mod. Phys. 44, 169 (1972).
[2]W. Gough, Proc. Phys. Soc., London 90, 287 (1967).
[3]F. D. Colegrove, L. D. Schearer, and G. K. Walters, Phys. Rev. 132, 2561 (1963).
[4]G. A. Ruff and T. R. Carver, Phys. Rev. Lett. 15, 282 (1965).
[5]R. B. Partridge and G. W. Series, Proc. Phys. Soc., London 88, 983 (1966).
[6]L. D. Schearer and L. A. Riseberg, Phys. Rev. Lett. 26, 599 (1971).
[7]W. Hanle, Z. Phys. 30, 93 (1924).

Evidence for Different Interaction Potentials for He^4-He^4 and He^3-He^3 from Scattering Cross-Section Measurements

H. G. Bennewitz, H. Busse, H. D. Dohmann, D. E. Oates,† and W. Schrader
Physikalisches Institut der Universität Bonn, Bonn, Germany
(Received 19 May 1972)

By means of low-energy cross-section measurements on He^3-He^3, we derive an interatomic potential which has a minimum 3.4% deeper than that of He^4-He^4. We demonstrate that the difference in the potentials is significant. The atomic-mass polarization effect is proposed as a possible explanation for the different potentials.

Recently, the He^4-He^4 atomic interaction has been determined very accurately by means of scattering measurements.[1,2] It is now possible to observe mass-dependent effects in the potential, which hitherto have not been included in theoretical calculations and have not been predicted. Furthermore, the helium system is especially interesting because of the effects of quantum statistics (He^4 is a boson with spin 0, and He^3 is a fermion with spin $\frac{1}{2}$). The cross section as a function of velocity shows an undulation structure due to the statistics, and the functional dependence of the cross section versus velocity is completely different for the two systems even for identical interaction potentials. Figure 1 shows the theoretical total scattering cross sections $Q(g)$ for He^4-He^4 and He^3-He^3 calculated from potentials explained below, with application of the proper particle statistics and mass.

In this Letter we present the results of measurements of the system He^3-He^3. We have already reported measurements of the system He^4-He^4 (Ref. 1); a description of the apparatus and the evaluation procedure will be found there. Figure 2 shows a part of the He^4-He^4 measurements along with the results of the measurements

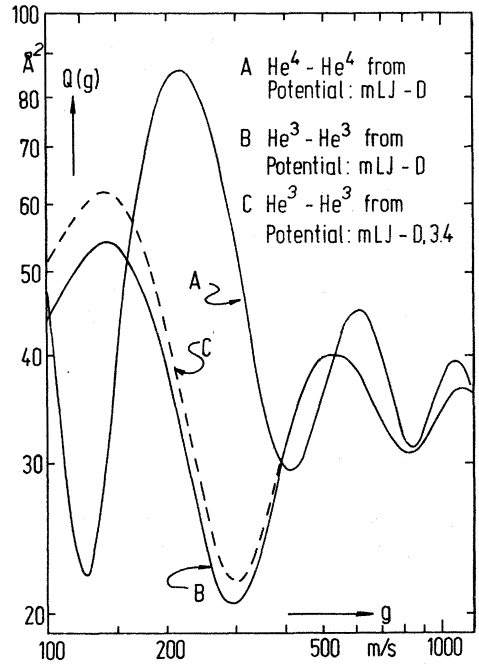

FIG. 1. Theoretical cross sections $Q(g)$ versus relative velocity g, calculated for different helium isotopes with two different potentials as shown. Curves B and C are essentially identical for $g > 400$ m/sec.

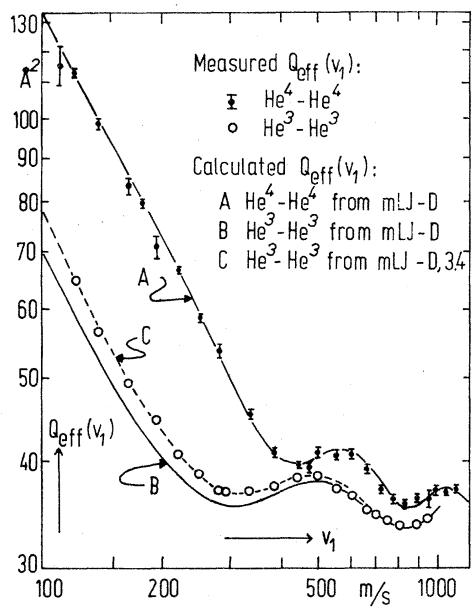

FIG. 2. Measured and calculated $Q_{eff}(v_1)$ as shown; v_1 is the beam velocity. Scattering chamber temperature is 5.0 K. The error bars for the He^4-He^4 measurements correspond to 1 standard deviation. The 1-standard-deviation errors for the He^3-He^3 measurements are smaller than the circles and are $< 0.8\%$.

for He^3-He^3. The He^3-He^3 and He^4-He^4 measurements are relative measurements with errors given in Fig. 2. We have, moreover, carried out an additional absolute calibration, with lower accuracy than the individual relative points, with the result that each set of measured points may be shifted as a whole by only $\pm 3.0\%$.[3] For reasons discussed below, the He^4-He^4 points shown in Fig. 2 have been shifted -0.6%, and the He^3-He^3 points $+2.5\%$. The solid lines in Fig. 2 are $Q_{eff}(v_1)$ as calculated by averaging $Q(g)$ over the proper velocity distributions of the beam and scattering gas. The $Q(g)$ in turn is calculated from the mLJ-D potential given in detail by the following expression[4,5]:

$$\begin{aligned}&\text{MDD-2 for } r \leq 2.15 \text{ Å},\\ &\text{LJ}(m_1, 6) \text{ for } 2.15 \text{ Å} \leq r \leq r_0,\\ &\text{LJ}(m_2, 6) \text{ for } r_0 \leq r \leq 6.3 \text{ Å},\\ &-(C_6/r^6 + C_8/r^8) \text{ for } r \geq 6.3 \text{ Å},\end{aligned}$$

with $\epsilon = 0.888$ meV, $r_0 = 2.685$ Å, $m_1 = 8.8$, and $m_2 = 14.5$, and with

$$\text{LJ}(m, 6) = \left[\left(\frac{6}{m}\right)^{m/(m-6)} - \left(\frac{6}{m}\right)^{6/(m-6)}\right]^{-1} \epsilon\left[\left(\frac{r_0}{r}\right)^m - \left(\frac{r_0}{r}\right)^6\right].$$

This potential is able to describe all existing He^4-He^4 scattering measurements.

Figure 2 shows clearly the influence of the different particle statistics. The figure also shows that the potential which has been deduced from He^4-He^4 measurements provides a poor fit to the He^3-He^3 data. However, when we enlarge ϵ by 3.4% leaving the other parameters unchanged, we arrive at an excellent fit to the He^3-He^3 measurements. $Q_{eff}(v_1)$ calculated from this potential, mLJ-D, 3.4, is shown by the dashed line in Fig. 2. Although 3.4% in ϵ is a rather small change in the potential, it is a significant difference in this case because these measurements are very sensitive with regard to changes of one of the parameters of the potential function. A look at Fig. 2 should give one an idea of the significance of the change in ϵ. Table I summarizes the situation with the use of χ^2 sums.[6] As seen in the table, the χ^2 sum for the He^3-He^3 measurements, using the He^4-He^4 best-fit potential, has a value which has a statistical probability of less than 0.001, and the He^4-He^4 measurements, using the He^3-He^3 potential, also have a χ^2 sum associated with a probability of less than 0.001. Furthermore, for both sets of measurements there is a range of ϵ values, centered on the ϵ values given in Table I, which give χ^2 sums associated with allowable statistical probabilities, but these ranges do not

TABLE I. ϵ values, χ^2 sums, and probabilities for the two sets of measurements with the two potentials given in the text.

Potential	ϵ (meV)	χ^2 sum He^4-He^4	χ^2 sum He^3-He^3	Statistical probability from χ^2 table He^4-He^4	Statistical probability from χ^2 table He^3-He^3
mLJ-D	0.888	23.4	350	0.5	$\ll 0.001$
mLJ-D, 3.4	0.918	105	19.6	$\ll 0.001$	0.5

overlap. Figure 3 shows the bands of He^4-He^4 and He^3-He^3 potentials produced by ϵ values which give χ^2 sums whose associated probabilities are >0.01. The best-fit potential for each set of measurements is shown in the middle of each band. With high statistical significance the bands do not overlap.

We have made a thorough study of the potentials which fit our He^4-He^4 measurements,[1] in that we have investigated the effects of variations of all of the parameters (ϵ, r_0, and the exponents of the LJ expression) and found a family of potentials which fit our measurements. The ranges of the parameters are given by the following: $0.786 < \epsilon < 0.926$ meV, $2.59 < r_0 < 2.72$ Å, $16.6 > m_1 > 6.8$, and $10.2 < m_2 < 17.0$. (The choice of one of these parameters determines the other three.) However, *each* potential which fits our He^4-He^4 measurements *fails* to fit the He^3-He^3 measurements, while an enlargement of ϵ by a factor between 1.03 and 1.04, depending on the potential, provides an excellent fit in each case.[7] Although we are naturally not able to give a mathematical proof that no single potential can exist which simultaneously fits both sets of measurements, we conclude that the interaction potentials for the two helium systems are different and He^3-He^3 has a $(3.5 \pm 0.5)\%$ stronger interaction than He^4-He^4.

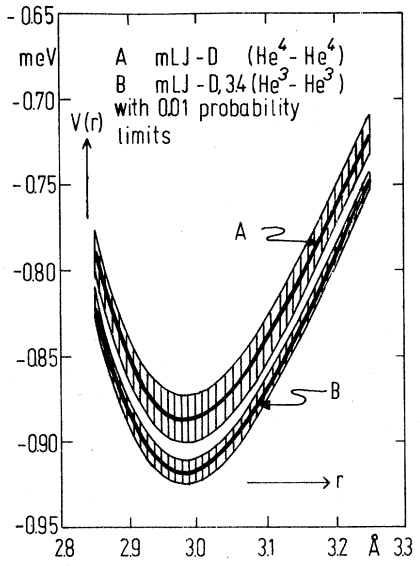

FIG. 3. Region of the potential minimum. This shows the effects of ϵ variations. Other parameters are held constant. Potentials in the bands correspond to χ^2 sums associated with statistical probabilities >0.01. The potentials which provide the best fit to the measurements are shown by the heavy lines in the middle of each band.

Due to the lack of theoretical calculations on the subject, an explanation of the different potentials is difficult to offer. A possibility, however, would be the so-called mass polarization effect.[8] This is the largest mass-dependent term in the atomic interaction and has been neglected in *ab initio* calculations.[9] The mass polarization term has been calculated for H-H and D-D systems.[10] Using these calculated values, a crude estimate shows that the He^3-He^3 potential could be as much as 5% stronger than the He^4-He^4 potential. Exact calculations of the mass polarization term are unfortunately not available.

We would like to thank W. aufm Kampe for his extensive help with the measurements and data analysis, and R. Gengenbach for the computer program with which the entire data analysis was carried out.

---

*Research supported by the Deutsche Forschungsgemeinschaft.

†Alexander von Humboldt-Stiftung Fellow.

[1]H. G. Bennewitz, H. Busse, H. D. Dohmann, D. E. Oates, and W. Schrader, Z. Phys. 253, 435 (1972).

[2]P. Cantini, M. G. Dondi, G. Scoles, and F. Torello, J. Chem. Phys. 56, 1946 (1972); P. E. Siska, J. M. Parson, T. P. Schafer, and Y. T. Lee, J. Chem. Phys. 55, 5762 (1971); R. Gengenbach, C. Hahn, and W. Welz, to be published.

[3]In Ref. 1 these He^4-He^4 measurements were reported as relative measurements. The absolute calibration was made for the He^3-He^3 measurements, and thus the He^4-He^4 measurements are now also fixed in absolute

value.

[4]L. W. Bruch and I. J. McGee, J. Chem. Phys. 52, 5884 (1970).

[5]W. D. Davison, Proc. Phys. Soc., London 87, 133 (1966).

[6]The χ^2 sum is defined by

$$\chi^2=\sum_{i=1}^{N}\frac{[Q_{\mathrm{eff}}{}^{m}(v_{1i})-Q_{\mathrm{eff}}{}^{\mathrm{th}}(v_{1i})]^2}{[\Delta Q_{\mathrm{eff}}(v_{1i})]^2},$$

where $Q_{\mathrm{eff}}{}^{m}(v_{1i})$ are the measured points, $\Delta Q_{\mathrm{eff}}(v_{1i})$ are the errors of the measured points, and $Q_{\mathrm{eff}}{}^{\mathrm{th}}(v_{1i})$ are the calculated values.

[7]We observed that each potential which gives a good fit to the He^4-He^4 measurements led, within 0.5%, to the same absolute cross section, which was well within the constraints on the absolute values of the measurements but not in the middle of the region. We have found it impossible to change the potential in such a manner that the calculated cross-section curve can be shifted to lie in the middle of the region of uncertainty and preserve the relative shape. Consequently, the measured points shown in Fig. 2 are shifted by the amount stated in the text to fit the theoretical curves.

[8]H. A. Bethe and E. E. Salpeter, in *Handbuch der Physik*, edited by S. Flügge (Springer, Berlin, 1957), Vol. 35, Part 1, p. 252; M. H. Mittleman, Phys. Rev. 188, 221 (1969).

P. Bertoncini and A. C. Wahl, Phys. Rev. Lett. 25, 991 (1970); H. F. Schaefer, D. R. McLaughlin, F. E. Harris, and B. J. Alder, Phys. Rev. Lett. 25, 988 (1970).

[10]A. Frőman, J. Chem. Phys. 36, 1490 (1962).

Observation of Resonance Raman Scattering below the Dissociation Limit in I_2 Vapor*

D. G. Fouche† and R. K. Chang
Department of Engineering and Applied Science, Yale University, New Haven, Connecticut 06520
(Received 13 June 1972)

Inelastic photon scattering from I_2 vapor was observed to change from resonance Raman scattering to resonance fluorescence as a single-mode argon laser was tuned through the 5145-Å gain profile. 3 orders of magnitude enhancement in the Stokes and the first-overtone intensities were measured in going from resonance Raman scattering to resonance fluorescence. The intensity distribution of the first 47 overtones is shown for the laser frequency coincident with the $43\rightarrow 0$ $P(12)$ and $43\rightarrow 0$ $R(14)$ transitions of $B^3\Pi_{0u}{}^+\rightarrow X^1\Sigma_{0g}{}^+$. The resonance Raman cross section of I_2 compared with N_2 was found to be 2.6×10^6.

The fortunate coincidence of the 5145-Å argon-laser emission with several optical transitions of I_2 vapor[1] [$43\rightarrow 0$ $P(12)$ and $43\rightarrow 0$ $R(14)$ of $B^3\Pi_{0u}{}^+\rightarrow X^1\Sigma_{0g}{}^+$] has stimulated investigations in the resonance fluorescence (RF) by using single-mode laser excitation, tunable over the 5145-Å Doppler gain profile.[2,3] Studies of RF of I_2 vapor have also been carried out by using multimode lasers[1,4,5] that have photon energies below the I_2 dissociation limit. However, resonance Raman scattering (RRS) from I_2 has been observed[6-8] only when the laser photon energies are above the I_2 dissociation limit. Excitation into the absorption continuum complicates RRS theories,[9-11] as one needs to include both discrete and continuum states. In this Letter, we report the first observation of RRS in a gas below its dissociation limit.

Inelastic photon scattering from I_2 vapor was observed to change from RRS to RF as the single-mode argon-laser frequency was tuned through the 5145-Å gain profile. Associated with this change from RRS to RF, the scattered intensity of the Stokes line and the first overtone was enhanced by 3 orders of magnitude. The cross section of I_2 in the resonance Raman case is found to be over 6 orders of magnitude larger than the Raman cross section of N_2 gas. Also associated with the transition from RRS to RF, the spectrum of the scattered radiation was observed to be markedly different.

The transitions[6] from ordinary Raman scattering (ORS) to RRS, then to RF, and finally back to RRS when the incident photon energy is above the continuum limit, are of basic theoretical interest in solids,[12] liquids,[13] and gases, as well as of practical significance in the possible use of laser backscattering for remote monitoring of air pollutants.[14] Since a significant amount of I_2 vapor is liberated by marine organisms to the atmosphere at the ocean surface, the presence of I_2 vapor can potentially be used as an indicator of marine bioproductivity.[15] Recently I_2 vapor has been used as a resonance filter for Raman scattering experiments[16] and has been proposed as a